frontiers | Frontiers in Ecology and Evolution

ORIGINAL RESEARCH
published: 06 June 2022
doi: 10.3389/fevo.2022.894471

Pollen-Based Holocene Thawing-History of Permafrost in Northern Asia and Its Potential Impacts on Climate Change

*Wenjia Li[1,2], Fang Tian[3], Natalia Rudaya[4,5], Ulrike Herzschuh[6,7,8] and Xianyong Cao[1]**

[1] Group of Alpine Paleoecology and Human Adaptation (ALPHA), State Key Laboratory of Tibetan Plateau Earth System, Resources and Environment (TPESRE), Institute of Tibetan Plateau Research, Chinese Academy of Sciences, Beijing, China, [2] University of Chinese Academy of Science, Beijing, China, [3] College of Resource Environment and Tourism, Capital Normal University, Beijing, China, [4] PaleoData Lab, Institute of Archaeology and Ethnography SB RAS, Novosibirsk, Russia, [5] Biological Institute, Tomsk State University, Tomsk, Russia, [6] Polar Terrestrial Environmental Systems, Alfred Wegener Institute Helmholtz Centre for Polar and Marine Research, Potsdam, Germany, [7] Institute of Environmental Science and Geography, University of Potsdam, Potsdam, Germany, [8] Institute of Biochemistry and Biology, University of Potsdam, Potsdam, Germany

OPEN ACCESS

Edited by:
Laurent Marquer,
Max Planck Institute for Chemistry, Germany

Reviewed by:
Heikki Tapani Seppä,
University of Helsinki, Finland
Rachid Cheddadi,
Université de Montpellier, France

***Correspondence:**
Xianyong Cao
xcao@itpcas.ac.cn

Specialty section:
This article was submitted to Paleoecology, a section of the journal Frontiers in Ecology and Evolution

Received: *11 March 2022*
Accepted: *03 May 2022*
Published: *06 June 2022*

Citation:
Li W, Tian F, Rudaya N, Herzschuh U and Cao X (2022) Pollen-Based Holocene Thawing-History of Permafrost in Northern Asia and Its Potential Impacts on Climate Change. Front. Ecol. Evol. 10:894471. doi: 10.3389/fevo.2022.894471

As the recent permafrost thawing of northern Asia proceeds due to anthropogenic climate change, precise and detailed palaeoecological records from past warm periods are essential to anticipate the extent of future permafrost variations. Here, based on the modern relationship between permafrost and vegetation (represented by pollen assemblages), we trained a Random Forest model using pollen and permafrost data and verified its reliability to reconstruct the history of permafrost in northern Asia during the Holocene. An early Holocene (12–8 cal ka BP) strong thawing trend, a middle-to-late Holocene (8–2 cal ka BP) relatively slow thawing trend, and a late Holocene freezing trend of permafrost in northern Asia are consistent with climatic proxies such as summer solar radiation and Northern Hemisphere temperature. The extensive distribution of permafrost in northern Asia inhibited the spread of evergreen coniferous trees during the early Holocene warming and might have decelerated the enhancement of the East Asian summer monsoon (EASM) by altering hydrological processes and albedo. Based on these findings, we suggest that studies of the EASM should consider more the state of permafrost and vegetation in northern Asia, which are often overlooked and may have a profound impact on climate change in this region.

Keywords: pollen, Random Forest, Siberia, East Asian summer monsoon, permafrost

INTRODUCTION

Permafrost is defined as ground that remains entirely frozen for at least two consecutive years (Washburn, 1973; Brown et al., 2002). It occurs across approximately 17% of the Earth's land surface and 24% of the Northern Hemisphere land (Zhang et al., 1999), and is highly vulnerable to the increasing global temperature. With the background of global warming, it is indisputable that the permafrost is thawing and will further degrade in the future (Intergovernmental Panel on Climate Change, 2013, 2019; Biskaborn et al., 2019), especially at high latitudes, where temperatures have risen more than average due to polar amplification (Miller et al., 2010). As a carbon reservoir, permafrost will release greenhouse gases, such as CO_2 and CH_4, as it thaws, which will enhance the greenhouse effect and therefore produce a positive feedback to climate warming (Knoblauch et al., 2018; Natali et al., 2021). Permafrost thawing also changes hydrology and geomorphology, such as the development of thermal karstification, coastline erosion, and liquefaction of the ground, affecting a wide range of permafrost regions (Anisimov and Reneva, 2006). Estimating the extent of permafrost degradation has become a vital component of predicting future warming.

Since the observational record is insufficient to meet our understanding of permafrost degradation (temporal restriction; Boike et al., 2019; Vasiliev et al., 2020), the challenge is how to capture the long-term behavior of permafrost in response to changing climate. Scrutinizing past permafrost variability during a long-term period may provide us with a useful insight into the potential conditions of permafrost in the future. However, palaeo-permafrost and palaeo-periglacial evidence, which can directly reveal the formation and development of past permafrost, is not easily found and has been subjected to various controversial interpretations (Jin et al., 2019). Several proxies such as the formation history of speleothems and thermokarst lakes have been used to reconstruct the evolution of past permafrost (Vaks et al., 2013, 2020; Brosius et al., 2021; Li et al., 2021), but due to the scarcity of research materials, these proxies are inevitably problematic in the continuity of space-time distribution and quantitative research. Therefore, other suitable indicators to reconstruct past permafrost conditions are desirable. In previous permafrost reconstruction, pollen, as one of the most common and mature proxies in investigating past vegetation changes, was often only used as a supplementary means to judge the status of regional permafrost conditions by reconstructing palaeo-temperature and palaeo-flora (Streletskaya et al., 2013; Jin et al., 2019). Although the high variability of the modern vegetation cover over the entire Asian continent, over the long course of geological and biological evolution, an ecological balance has been formed between vegetation and permafrost (Chang et al., 2012), and some plants can be used as indicators of permafrost in different area (Brown, 1963; Tyrtikov, 1973; Black, 1976), such as larch-pumila forest and larch-*Ledum* forest in the Greater and Lesser Hinggan Mountains of China (Zhang, 1983), or the bryophyte forest in the northern taiga of western Siberia (Guo et al., 1998). Therefore, we can use pollen as a potential tool to track past permafrost and its relationship with global climate.

Current global warming is triggering a strong and rapid positive feedback to the phenomenon of greening in the Arctic (Elmendorf et al., 2012; Myers-Smith et al., 2020), but research at long-term scales has suggested that permafrost can cause a disequilibrium between vegetation and climate to persist for several millennia (Herzschuh et al., 2016), implying that, in addition to climate, vegetation changes are also subject to the extent and state of permafrost (Tchebakova et al., 2006). Thus, the question arises of whether the changes in vegetation and state of permafrost are the result of passive acceptance of the effects of climate change. Previous studies have shown that the interplay of climate, vegetation, and permafrost is complex. Under the warm and wet 127 ka climate, for example, a 10% increase in EASM precipitation in the dry region in north China contributed to vegetation feedback (Zhang and Chen, 2020). A numerical simulation model also confirms that changes in the global frozen soil have profound impacts on the East Asian climate (Xin et al., 2012).

As an important part of the global climate system, the fluctuation in EASM intensity will influence the distribution of precipitation and the evolution of the ecological environment in the monsoon region (Wang, 2006; Clift and Plumb, 2008) – a topic that has been extensively studied at a suborbital scale (Xiao et al., 2004; Chen et al., 2015; Liu et al., 2015; Kang et al., 2020; Xu et al., 2020). These studies unanimously find that there is a lag (∼4 ka) between EASM intensity and solar radiation in the early Holocene. Although this lag is generally considered to be related to the decrease of the Northern Hemisphere land-ice volume, associated with the weakening of the Atlantic meridional overturning circulation (Barber et al., 1999; Carlson et al., 2008; Yu et al., 2010), much of the research focuses on ice sheets in North America and Europe, discarding northern Asia, particularly Siberia and the central and northern Mongolia regions, which have abundant ice stored underground in the form of permafrost (Karlsson et al., 2012; Wang et al., 2021).

Here, we constructed a Random Forest (RF) model using modern pollen data and permafrost distribution in northern Asia, and then applied the trained model to reconstruct the permafrost history of the late Quaternary based on fossil pollen data (Cao et al., 2020). The objectives of this study are to (1) assess the relationship between pollen and permafrost and the reliability of the trained model; (2) reveal the permafrost changes in northern Asia during the Holocene; and (3) explore the potential impact of variations in the permafrost on the early-to-middle Holocene East Asian monsoon system.

DATA AND METHODS

Pollen and Permafrost Data

A total of 2,212 modern pollen assemblages published previously (**Figure 1**) for northern continental Asia (east of 50°E and north of 45°N) are included in our analyses: most of them are extracted from topsoil, moss samples, or lake core-top samples. The Chinese and Mongolian modern pollen data primarily come from Cao et al. (2014), while Siberian data primarily come from Bordon et al. (2009) and Natalia et al. (2020). Other data include records for the northern and central Yakutia (Müller et al., 2010), the Russian Far-East (Tarasov et al., 2011), and the Khatanga River region (Niemeyer et al., 2015; Klemm et al., 2016). The fossil pollen records (**Figure 1**) were obtained from lacustrine sediments and peat from the same area of northern Asia, and comprise 6,873 fossil pollen assemblages from 199 records (Cao et al., 2020). For these modern and fossil pollen data, pollen names were taxonomically harmonized at the family or genus level generally and pollen percentages were re-calculated based on the total number of terrestrial pollen grains, following the method described by Cao et al. (2013, 2020). Based on calibrated radiocarbon dates, an age-depth model was established for each record using a Bayesian approach (further details are described in

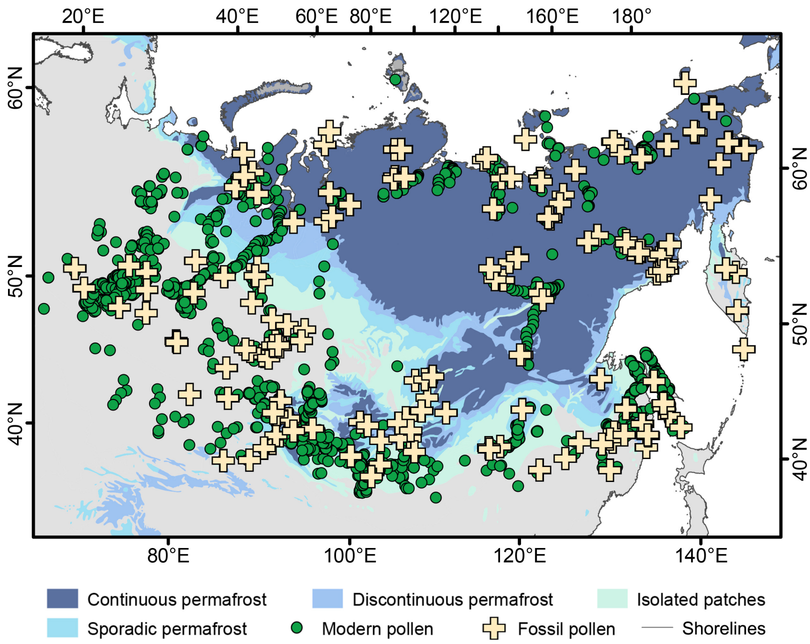

FIGURE 1 | Distribution of the 2212 modern pollen sites (green circles) together with the 199 fossil record sites (beige crosses) and permafrost extent in northern Asia.

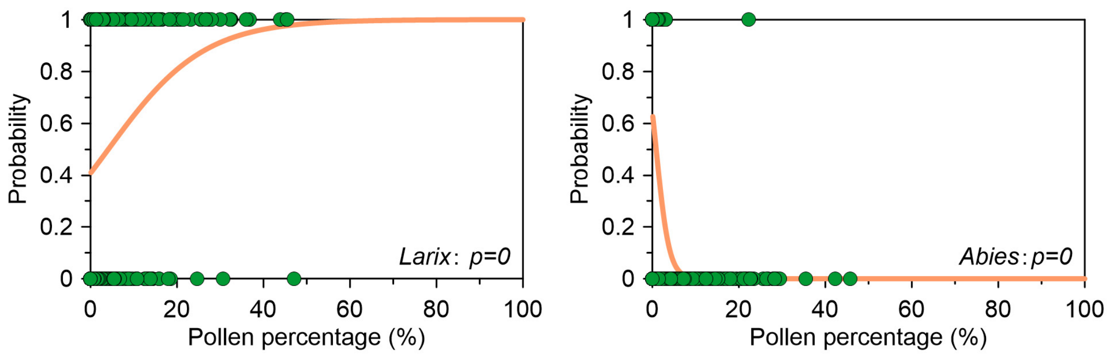

FIGURE 2 | Logistic regression curves for *Larix* and *Abies*.

TABLE 1 | Summary of the Random Forest training runs.

	Accuracy	Kappa
Run 1	0.84	0.76
Run 2	0.84	0.76
Run 3	0.83	0.75
Mean	0.84	0.76

Cao et al., 2013). In this study, we selected records between 12.5 and 0 cal ka BP, covering the Holocene.

Modern permafrost data was downloaded from the open database Circum-Arctic Map of Permafrost and Ground-Ice Conditions (version 2) (Brown et al., 2002), which maps the distribution of permafrost in the Northern Hemisphere from 20°N to 90°N. Based on the estimated percentage of area, the permafrost extent is divided into continuous permafrost (90–100%), discontinuous permafrost (50–90%), sporadic permafrost (10–50%), isolated patches (<10%), and no permafrost. For easier classification, we merged the three transitional states between continuous permafrost and no permafrost into one category of non-continuous permafrost. The resulting three states of continuous permafrost, non-continuous permafrost, and permafrost-free are used throughout our research. Using this distribution map of permafrost, conditions prevailing at the modern pollen sites are assigned.

Modeling the Response of Permafrost to Pollen Taxa

We fitted a logistic regression model to estimate the probability of the presence of permafrost in northern Asia by relating modern

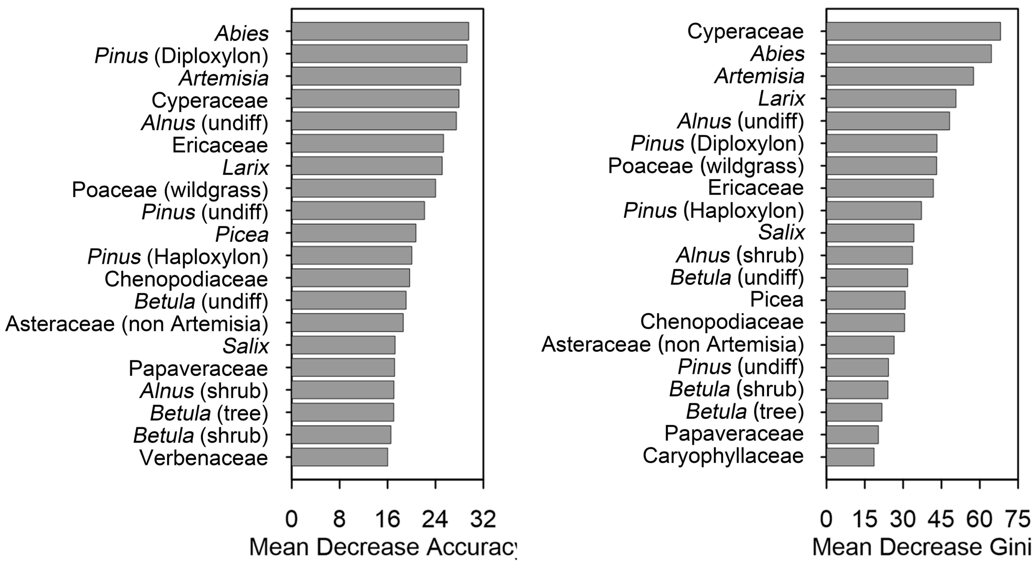

FIGURE 3 | Importance of pollen taxa in pollen-based permafrost classification model for test-set measured by the Mean Decrease Accuracy and Mean Decrease Gini.

TABLE 2 | Summary of precision and recall rate for the classification of permafrost state.

	Continuous permafrost	Non-continuous permafrost	Permafrost-free
Precision	0.90	0.79	0.83
Recall	0.88	0.79	0.84

pollen percentages from 74 pollen taxa shared by modern and fossil pollen records to the permafrost data. To obtain more reliable regression results, we only selected samples from regions with permafrost-free and continuous permafrost. The association between the pollen percentage (predictor variable) and the presence of permafrost (response variables) was assessed by the Wald test. A p-value less than 0.05 is considered statistically significant. The logistic regression was implemented using the *glm* function in the *stats* package in R version 4.0.3 (R Core Team, 2020).

Random Forest

Random Forest is a machine-learning algorithm that can be used to solve regression and classification problems (Breiman, 2001). RF operates by constructing a multitude of decision trees. Although factors such as the number of trees in RFs may bias the regression results to some extent (Strobl et al., 2007; Arlot and Genuer, 2014), RFs have been successfully used in the field of earth science to predict future species distributions, and to reconstruct local and even global past tree species distributions (Prasad et al., 2006; Benito Garzón et al., 2007; Lindgren et al., 2021; Qin, 2021).

Our RF model was trained on 74 pollen taxa from the 2,212 modern samples that were matched to permafrost conditions. For the 2,212 samples, 70% of samples served as the training set for RF, while the remaining 30% of samples served as a test-set. We conducted three separate training runs using RF to assess the stability of the model and selected the training model with the highest overall statistical accuracy and Kappa value. The trained RF was then applied to down-core palynological records from 199 boreholes, sampled in northern Asia to reconstruct past permafrost conditions. These steps were implemented collectively using the R version 4.0.3 built-in package *randomForest* (version 4.6-14; Liaw, 2018).

RESULTS

Response of Different Pollen Taxa to Permafrost

Pollen data from topsoil together with current permafrost extent offer a unique opportunity to understand the relationship between the presence of permafrost and the occurrence of specific pollen taxa. Among the 74 pollen taxa analyzed, 20 taxa significantly correlate with the presence of permafrost ($P < 0.05$). *Alnus* (shrub), *Betula* (shrub), *Larix*, and another 13 taxa are positively correlated with the presence of permafrost, while *Abies*, *Pinus* (Diploxylon), *Picea,* and another 7 taxa are negatively correlated with the presence of permafrost (**Supplementary Figure 1**). Using *Larix* and *Abies* as examples, the probability of permafrost being present increases as the percentage of *Larix* pollen increases but decreases as the percentage of *Abies* pollen decreases (**Figure 2**). This suggests that the variability of pollen taxa can reflect shifts between the presence or absence of permafrost and thus be used to reconstruct permafrost conditions.

Random Forest Performance

Based on assessments of the test-sets of three separate training runs, the RF model has great stability with a mean accuracy of

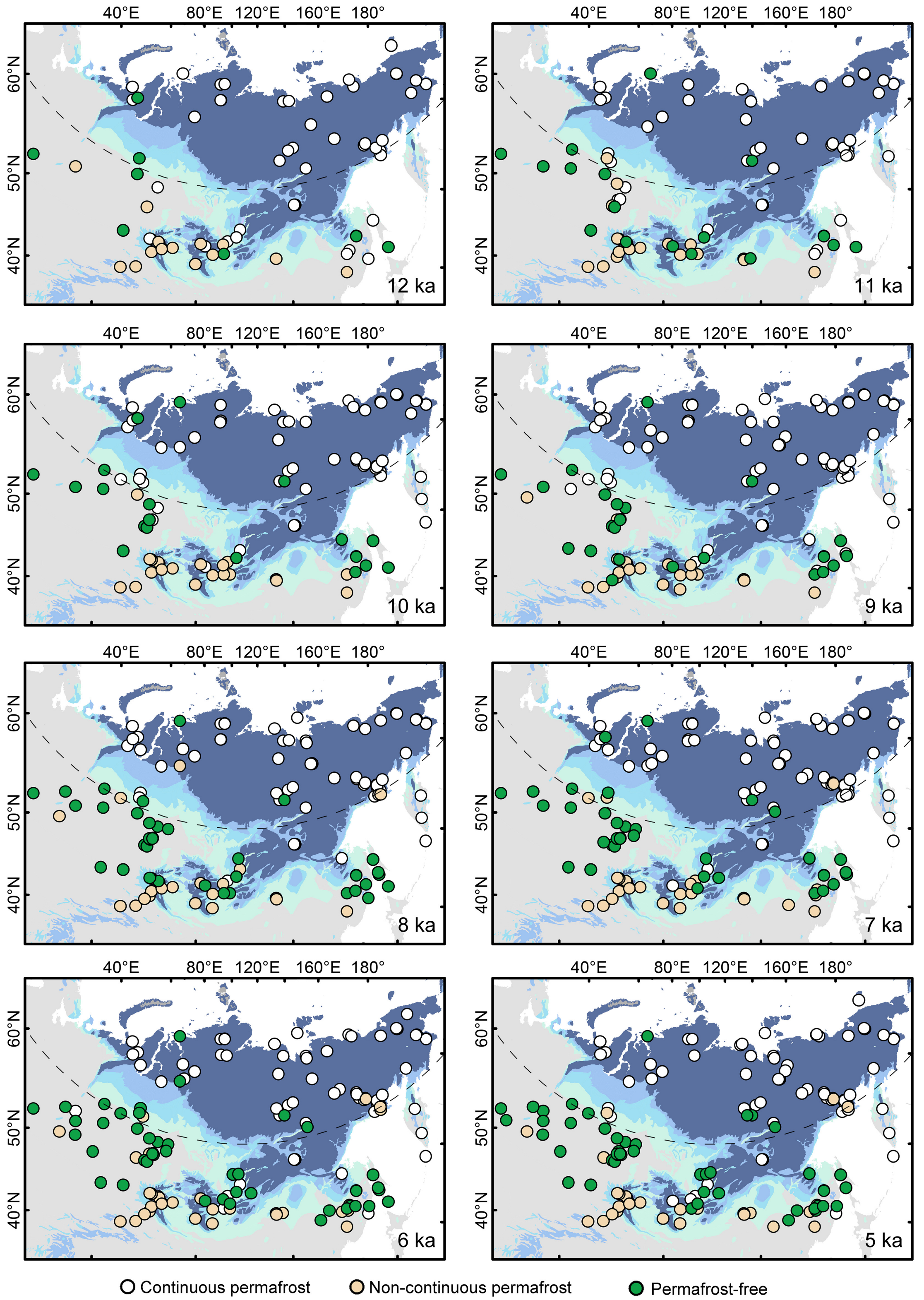

FIGURE 4 | Temporal and spatial changes in permafrost state (continuous permafrost: white circles; non-continuous permafrost: beige circles; permafrost free: green circles) reconstructed for northern Asia from 12 to 5 cal ka BP.

0.84 and a mean Kappa value of 0.76 (**Table 1**) and almost no variance between the runs. Mean Decrease Accuracy and Mean Decrease Gini of a taxon indicate the importance of that taxon to the accuracy of permafrost state classification. Of the 74 taxa used in our classification model, 30 had a Mean Decrease Accuracy value of more than 10 and 29 had a Mean Decrease Gini value of more than 10 (**Figure 3**). Obviously, these taxa play a key role in classifying the state of permafrost.

The precision and recall rate are two important statistical metrics to evaluate the classification quality, measuring the fraction of relevant instances among the retrieved instances and the fraction of relevant instances that were retrieved, respectively. The precision and recall rate of our RF classification for different states of permafrost differ slightly (**Table 2**) being best for continuous permafrost and worst for non-continuous permafrost.

Temporal and Spatial Variability of Permafrost Conditions

To gain an understanding of the overall condition in different time periods, we take the most frequently reconstructed state of each record in each 1000-year window. For different time slices of the Holocene, the distribution of permafrost changed significantly, especially in the early-to-middle Holocene (**Figure 4** and **Supplementary Figure 2**). From 12 to 5 cal ka BP, in addition to Asia north of 60°N, which is currently the main distribution area of continuous permafrost, the vast northern Asia region south of 60°N, such as the West Siberian Plain, southeastern Siberia, Lake Baikal region, and Kamchatka peninsula, sporadically experienced continuous permafrost state. Focusing on the West Siberian Plain, despite the widespread permafrost conditions before 9 cal ka BP, no continuous permafrost was reconstructed for this region at 7 cal ka BP. The main distribution of non-continuous permafrost between 12 and 5 cal ka BP is found in northern Asia south of 60°N, especially in the Tianshan-Altai region and the Mongolian Plateau region. However, there is no obvious spatial pattern in the distribution of sites with non-continuous permafrost. In contrast to the area north of 60°N, a permafrost-free state is frequently reconstructed from sites in the area south of 60°N. Additionally, on the West Siberian Plain between 9 and 7 cal ka BP, permafrost-free states increased significantly.

The percentages of the three states at different time slices portray the evolution of permafrost in northern Asia during the Holocene (**Figure 5**). Continuous permafrost is always the highest among the three states throughout the Holocene, ranging from 41.6 to 67.1%. Continuous permafrost clearly decreases in the early Holocene (12–8 cal ka BP), with the rate of decline slowing down after reaching 48.8% at 8 cal ka BP. A slight increase in this state is observed in the most recent 1 ka. The proportion of non-continuous permafrost ranges from 19.0 to 24.7%, with an average value of 21.5%. Although the proportion of non-continuous permafrost has a stable trend during the Holocene, there was a slight increase at 1 cal ka BP followed by a decrease. In corollary, the percentage of permafrost-free state shows a sharply increasing trend from 12 to 8 cal ka BP and a gradually increasing trend after 8 cal ka BP until the late Holocene when it decreased. The decrease during 2–1 cal ka BP is caused by the formation of more non-continuous permafrost, while the decrease during 1–0 cal ka BP is caused by an increase in continuous permafrost.

DISCUSSION

Reliability of Pollen-Based Permafrost Reconstructions

Reconstructing past permafrost conditions using pollen data is credible as confirmed by logistic regression and statistical metrics from test-set. The relationship between pollen taxa and permafrost has been identified by logistic regression, and the results presented here imply that we can reconstruct the history of permafrost using pollen data. Additionally, the high average accuracy (0.84) based on the test-set means that the state of permafrost down-core can be reconstructed with a reasonably low error, while the Kappa statistic (up to 0.76) also suggests a substantial classification quality of the RF model (Landis and Koch, 1977). The precision and recall rate of continuous permafrost reach 0.90 and 0.88, respectively, indicating a good ability of the model. Although some of the samples in the test-set were mismatched by our trained RF model, it is worth noting that these misallocated samples are mainly distributed in marginal regions where the permafrost is in a state of flux (**Supplementary Figure 3**) and the pollen taxa show transitional characteristics. Overall, the classification results of samples within the different permafrost states are very reliable.

The synchrony of changes in permafrost conditions with the Northern Hemisphere climatic signal and consistency with other permafrost proxies in northern Asia further support the reliability of pollen-based permafrost reconstructions (**Figure 6**). The freezing and thawing of permafrost have a close relationship to climate, and our reconstruction demonstrates the variation in permafrost state in northern Asia could depend on suborbital variations in summer solar insolation (Laskar et al., 2004). During the early Holocene, permafrost thawed rapidly (**Figure 6C**, from 12 to 8 cal ka BP), coinciding with a sharp increase in Northern Hemisphere temperature and North Atlantic air temperature after the Younger Dryas (**Figures 6A,B**; Andersen et al., 2004; Shakun et al., 2012; Marcott et al., 2013). After the northern hemisphere temperature reached a maximum in the middle Holocene, the rate of permafrost thawing in northern Asia slowed as the temperature and summer solar insolation decreased. The decreasing trend in proportion of permafrost-free during the late Holocene (**Figure 6D**) can also be explained by variation in the Northern Hemisphere temperature anomalies (**Figure 6B**). Continuous permafrost expanded during 2–0 cal ka BP when the stacked temperature anomalies show a return to under 0°C. The temporal and spatial variation of permafrost in western Siberia is very significant, which is consistent with the traditional research results of permafrost. Research on the palaeo-permafrost and palaeo-periglacial evidence shows that the severe freezing conditions that developed during Last Glacial time persisted of western Siberia in early Holocene, but until the

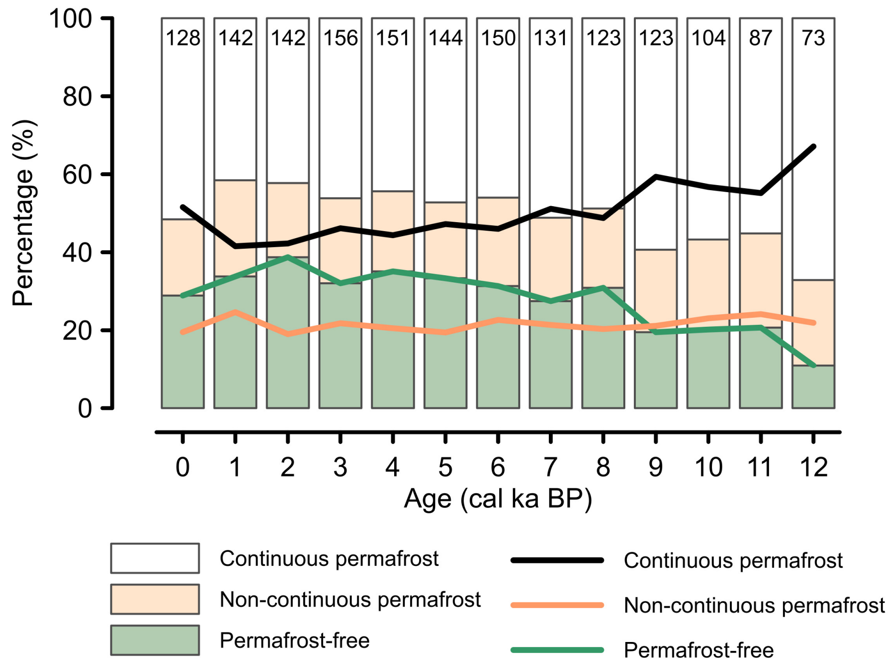

FIGURE 5 | Temporal variation of relative extent of permafrost state in northern Asia (the numbers on the bars indicate the number of samples).

Holocene optimum (7.5–4 cal ka BP), the southern boundary of surficial permafrost receded northward to near the Arctic Circle (**Supplementary Figure 4**; Velichko et al., 1984). Additionally, thermokarst lake formation history (**Figure 6H**), which can indicate permafrost degradation on a large scale, has recently been published for northern mid- to high-latitudes (Brosius et al., 2021) and the result of northern Asia suggests a rapid permafrost thawing period during the early Holocene (12–8 cal ka BP) and a relatively slow decreasing rate of thaw in the mid-late Holocene (7–2 cal ka BP): this result is consistent with our reconstruction based on pollen data.

Effect of Permafrost State on Vegetation in Northern Asia

A reanalysis of vegetation turnover (**Figure 7**), including evergreen conifer tree, summer-green conifer tree, summer-green broad-leaved tree, and non-tree vegetation from northern Asia based on pollen records (Cao et al., 2019) is instructive for our understanding of the relationship between permafrost and vegetation. Although an early-to-middle Holocene (12–7 cal ka BP) decreasing trend is observed in the non-tree vegetation component, the other vegetation components do not show a corresponding increasing trend. It was not until 8 ka that evergreen conifer species, dominated by pine and spruce, increased significantly, which is consistent with the increase of permafrost-free conditions. A re-analysis of the spatiotemporal distribution of the four vegetation types (**Figure 8**) shows that summer-green conifers (larch) were the main trees in northern Asia in the early Holocene, and the transition from summer-green conifer trees to evergreen conifer trees occurred around 8 cal ka BP, especially on the Western Siberian Plain (G2, G3, G8, G9), which coincided with the establishment of permafrost-free conditions.

It is reasonable to assume that the presence of permafrost in the early Holocene inhibited the spread of dark coniferous taiga. Despite increases in temperature, permafrost could not thaw deeply enough across Siberia to support dark coniferous taiga (dominated by pine) during the early Holocene. Traditional proxy-based climate reconstructions in the Northern Hemisphere suggest abrupt warming occurred at the onset of the Holocene, followed by a long-term cooling trend throughout the middle-to-late Holocene (Shakun et al., 2012; Marcott et al., 2013), which should be consistent with afforestation. However, the turnover of vegetation is not simply driven by changes in climate as traditionally thought, such as seed dispersal strategy of specific species (Travis et al., 2013), competition to the existing dominant vegetation (Meier et al., 2012), the existence of permafrost (Tian et al., 2018; Cao et al., 2019), and extensive fires (Schulze et al., 2012), which may affect the progress of plant migration. Research in northeast Asia has challenged the general view that the vegetation-climate lag is last no more than a few centuries, suggesting that during the Plio-Pleistocene, interglacial vegetation was influenced by the persistence of permafrost, mainly reflects conditions of the previous glacial period, lagging the climate by several millennia (Herzschuh et al., 2016). Therefore, compared with other non-permafrost regions, the extensive and deep permafrost in our study area, northern Asia, may have a profound impact on vegetation. Previous studies have demonstrated that larch can survive on permafrost with an active layer depth of less than 40 cm (Osawa et al., 2010), while pine requires at least 1.5 m of active layer to grow (Tzedakis and Bennett, 1995). In Alaska,

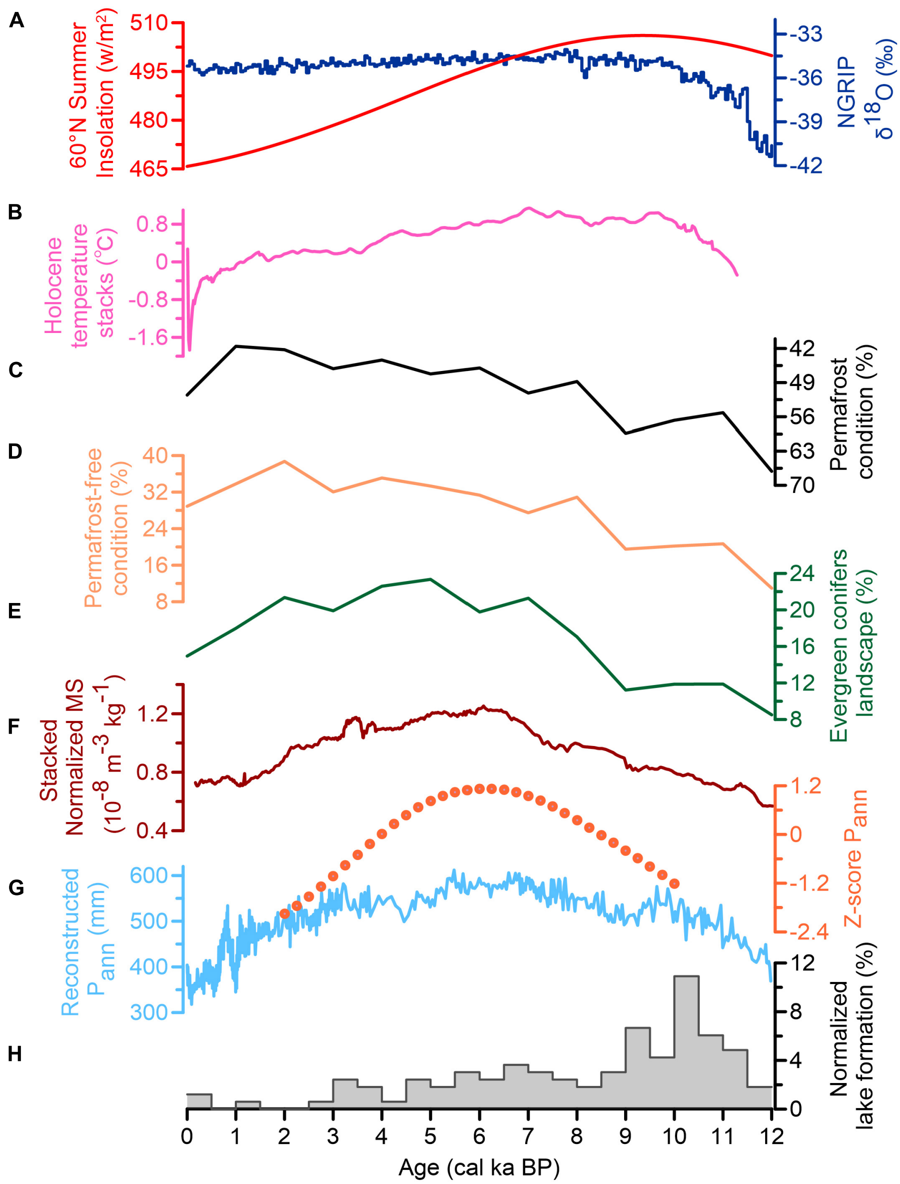

FIGURE 6 | Comparison of the northern Asian permafrost reconstruction with various other regional and global environmental signals. **(A)** 60°N summer insolation (red line, Laskar et al., 2004) together with North Greenland ice core $\delta^{18}O$ records indicative of North Atlantic air temperature (blue line, Andersen et al., 2004). **(B)** Northern Hemisphere temperature anomaly (Marcott et al., 2013). **(C)** Percentage of continuous permafrost reconstructed from Holocene pollen assemblages (this study). **(D)** Percentage of permafrost-free conditions reconstructed from Holocene pollen assemblages (this study). **(E)** Percentage of evergreen conifer tree taxa in Northern Asia (modified from Cao et al., 2019). **(F)** Stacked normalized magnetic susceptibility from Loess sections showing the intensity of the EASM (Kang et al., 2020). **(G)** Precipitation trends in north China during the Holocene (orange dots, Herzschuh et al., 2019) and reconstructed precipitation from Lake Gonghai in northern China (blue line, Chen et al., 2015). **(H)** Normalized frequency of lake formation in northern Asia (modified from Brosius et al., 2021).

permafrost with a shallow active layer is assumed to limit the northward extent of *Picea* (Lloyd, 2005). A pollen-based biochemical study also finds that during the early Holocene, only larch forests could survive on these shallow active-layer permafrost regions in northern Asia (Tian et al., 2018). A large amount of heat is needed to thaw permafrost and it takes time for deep permafrost to thaw (Galushkin, 1997; Vaks et al., 2013). However, our studies have not taken all relevant geoecological causal chains and their interactions into account. Our knowledge of permafrost and vegetation delay is thus still limited.

Potential Relationship Between Permafrost and the East Asian Summer Monsoon

The freezing and thawing of permafrost can change the hydrological processes, and the turnover in vegetation controlled

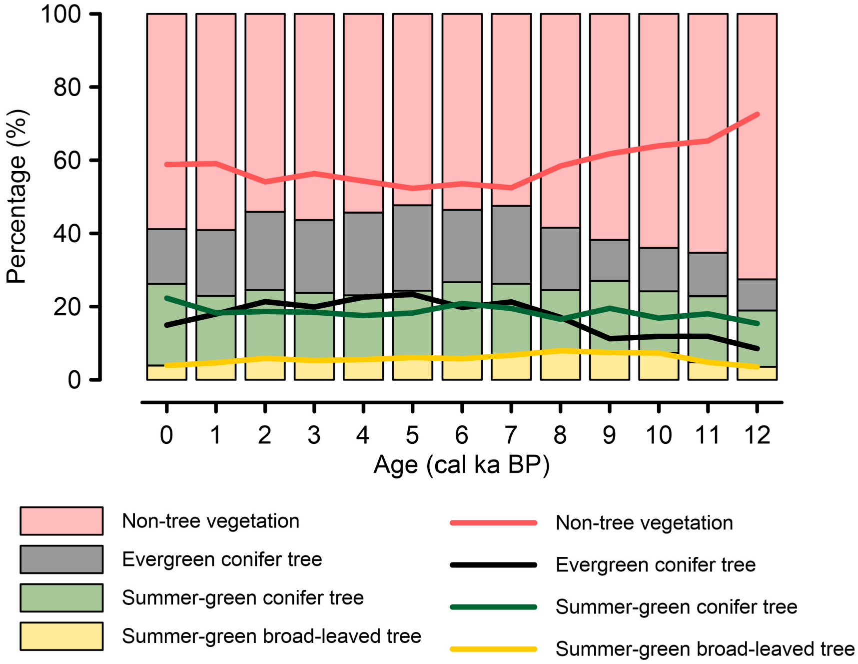

FIGURE 7 | Temporal variation in relative percentage of four vegetation types in northern Asia.

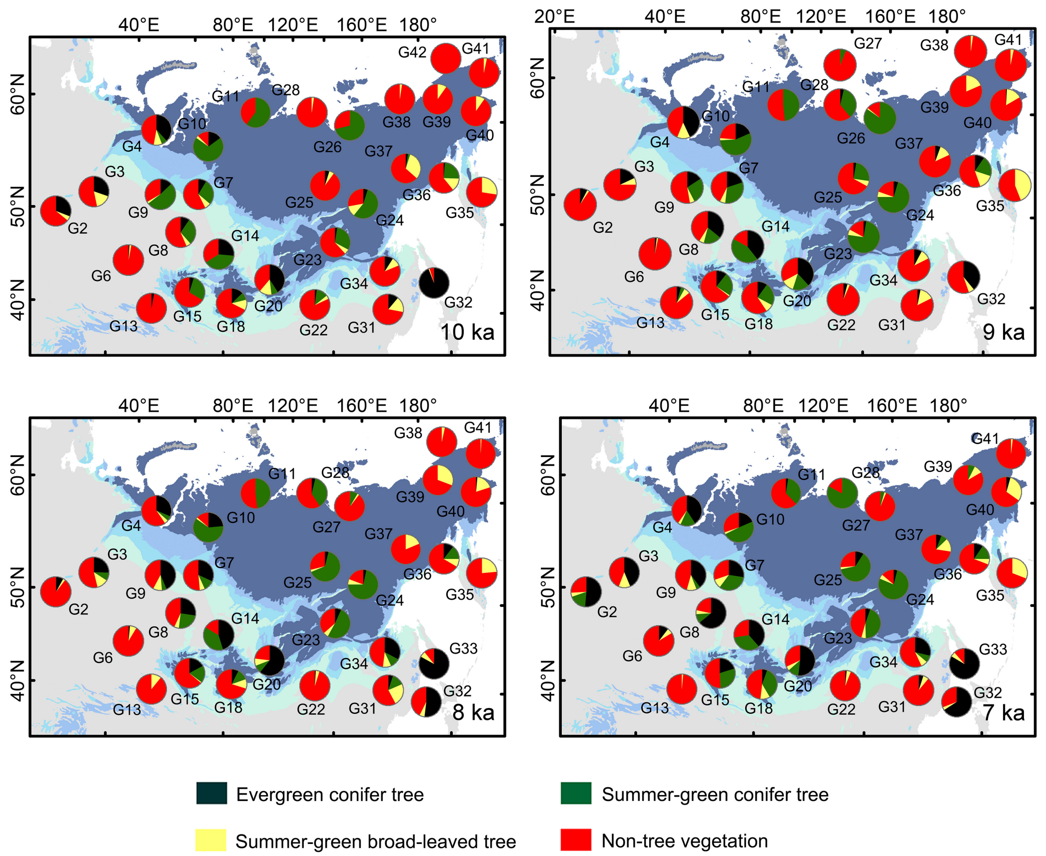

FIGURE 8 | Temporal changes in relative percentage of vegetation types for northern Asia during the early Holocene (10–7 cal ka BP; G*: site group; modified from Cao et al., 2019).

by permafrost could affect the land-surface albedo. The thawing of frozen soil will lead to changes in the ice/water ratio, altering the thermal and hydraulic qualities of the soil, and also affecting ground surface temperature (Xin et al., 2012). Numerical simulations with a supercooled soil-water model show that the thawing of frozen soil has a great impact on winter and spring soil moisture as well as temperature in Eurasia (Li et al., 2011; Xin et al., 2012). Landscapes with trees generally have a lower albedo than landscapes without trees and this difference may be magnified when there is snow cover. The albedo values of tundra and grassland when covered by fresh snow, can reach 0.76 and 0.65, respectively, while the average albedo value of three other vegetation types with trees is only 0.27 (Schaeffer et al., 2006). In addition, larch, being a deciduous coniferous species, lacks a canopy in winter and has a poor ability to cover snow compared to evergreens (Betts and Ball, 1997), with a peak winter albedo value of up to twice that of evergreen coniferous forest (dark taiga forest; Shuman et al., 2011).

A series of global atmospheric circulation models has suggested that the Eurasian snow cover has a significant effect on the Asian summer monsoon (Yang and Xu, 1994; Liu and Yanai, 2002; Wu et al., 2009; Xu et al., 2021), with a recent study showing that when there was excessive spring snowmelt in Siberia between 1981 and 2014, the EASM was weaker, resulting in less summer precipitation in north China (Xu et al., 2021). The inter-decadal variation of snow cover and summer monsoon can essentially be attributed to altered soil hydrology and albedo, which affect the surface and atmospheric temperature and soil moisture, leading to changes in thermal contrast and atmospheric circulation and thus regulating the intensity of the Asian summer monsoon rainfall (Cohen, 1994; Liu and Yanai, 2002; Jacob et al., 2005). Given the rapid thawing of permafrost and the high albedo caused by sparse evergreen coniferous trees in northern Asia during the early Holocene (**Figures 6C–E**), similar hydrological and atmospheric responses may have occurred, reducing the intensity of the early Holocene EASM (**Figure 6G**; Chen et al., 2015; Herzschuh et al., 2019; Kang et al., 2020). This mechanism, however, requires a mechanism model for further validation.

CONCLUSION

Reconstructed permafrost in northern Asia during the Holocene using an RF model based on pollen data largely corresponds with inferences from climate proxies and other permafrost reconstructions. Our reconstruction indicates a sharp thawing trend in the early Holocene (12–8 cal ka BP), a relatively slow thawing trend in middle-to-late Holocene (8–2 cal ka BP), and a freezing trend of permafrost after 2 cal ka BP in northern Asia. Additionally, permafrost degradation was clear on the West Siberian plain during 8–7 cal ka BP. The spatiotemporal consistency of the records of permafrost and evergreen coniferous trees variation suggests that the presence of permafrost in the early Holocene could inhibited the spread of vegetation. Furthermore, permafrost and permafrost-controlled vegetation types may affect the intensity of the EASM by influencing hydrological processes and albedo. This study reminds us that it is necessary to pay more attention to environmental factors in northern Asia, as they have potential impacts on climate change in the East Asian monsoon regions.

DATA AVAILABILITY STATEMENT

The raw data supporting the conclusions of this article will be made available by the authors, without undue reservation.

AUTHOR CONTRIBUTIONS

WL contributed to data analysis and interpretation, preparation of figures, and writing of the original draft. FT, NR, and UH contributed to the final version. XC conceived and conceptualized the idea, designed the work, contributed to data acquisition, analysis, wrote the manuscript, and supervised the study. All authors reviewed the manuscript.

FUNDING

This research was supported by the Basic Science Center for Tibetan Plateau Earth System (BSCTPES, NSFC project No. 41988101), CAS Pioneer Hundred Talents Program, and the Russian Science Foundation (project 20-17-00110).

ACKNOWLEDGMENTS

We gratefully acknowledge all those who made their pollen datasets available in databases for reanalysis in this research. Cathy Jenks provided help with language editing.

SUPPLEMENTARY MATERIAL

The Supplementary Material for this article can be found online at: https://www.frontiersin.org/articles/10.3389/fevo.2022.894471/full#supplementary-material

REFERENCES

Andersen, K. K., Azuma, N., Barnola, J.-M., Bigler, M., Biscaye, P., Caillon, N., et al. (2004). High-resolution record of northern hemisphere climate extending into the last interglacial period. *Nature* 431, 147–151. doi: 10.1038/nature02805

Anisimov, O., and Reneva, S. (2006). Permafrost and changing climate: the Russian perspective. *Ambio* 35, 169–175. doi: 10.1579/0044-7447(2006)35[169:pacctr]2.0.co;2

Arlot, S., and Genuer, R. (2014). Analysis of purely random forests bias. *arXiv* [Preprint]. arXiv:1407.3939.

Barber, D. C., Dyke, A., Hillaire-Marcel, C., Jennings, A. E., Andrews, J. T., Kerwin, M. W., et al. (1999). Forcing of the cold event of 8,200 years ago by catastrophic drainage of Laurentide lakes. *Nature* 400, 344–348. doi: 10.1038/22504

Benito Garzón, M., Sánchez de Dios, R., and Sáinz Ollero, H. (2007). Predictive modelling of tree species distributions on the Iberian Peninsula during the last glacial maximum and mid-Holocene. *Ecography* 30, 120–134. doi: 10.1111/j.0906-7590.2007.04813.x

Betts, A. K., and Ball, J. H. (1997). Albedo over the boreal forest. *J. Geophys. Res. Atmos.* 102, 28901–28909. doi: 10.1029/96JD03876

Biskaborn, B. K., Smith, S. L., Noetzli, J., Matthes, H., Vieira, G., Streletskiy, D. A., et al. (2019). Permafrost is warming at a global scale. *Nat. Commun.* 10:264. doi: 10.1038/s41467-018-08240-4

Black, R. (1976). Features indicative of permafrost. *Annu. Rev. Earth Planet. Sci.* 4, 75–94. doi: 10.1146/annurev.ea.04.050176.000451

Boike, J., Nitzbon, J., Anders, K., Grigoriev, M., Bolshiyanov, D., Langer, M., et al. (2019). A 16-year record (2002–2017) of permafrost, active-layer, and meteorological conditions at the Samoylov Island Arctic permafrost research site, Lena River delta, northern Siberia: an opportunity to validate remote-sensing data and land surface, snow, and permafrost models. *Earth Syst. Sci. Data* 11, 261–299. doi: 10.5194/essd-11-261-2019

Bordon, A., Peyron, O., Lézine, A.-M., Brewer, S., and Fouache, E. (2009). Pollen-inferred late-glacial and Holocene climate in southern Balkans (lake maliq). *Q. Int.* 200, 19–30. doi: 10.1016/j.quaint.2008.05.014

Breiman, L. (2001). Random forests. *Mach. Learn.* 45, 5–32. doi: 10.1023/A:1010933404324

Brosius, L. S., Anthony, K. M. W., Treat, C. C., Lenz, J., Jones, M. C., Bret-Harte, M. S., et al. (2021). Spatiotemporal patterns of northern lake formation since the last glacial maximum. *Q. Sci. Rev.* 253:106773. doi: 10.1016/j.quascirev.2020.106773

Brown, J., Ferrians, O., Heginbottom, J. A., and Melnikov, E. (2002). *Data from: Circum-Arctic Map of Permafrost and Ground-Ice Conditions, Version 2.* Boulder, CO: National Snow and Ice Data Center. doi: 10.7265/skbg-kf16

Brown, R. (1963). "Influence of vegetation on permafrost," in *Proceedings of the Permafrost International Conference*, eds K. B. Woods and A. J. Alter (Washington, DC: National Academy of Sciences-National Research Council), 20–25.

Cao, X., Tian, F., Andreev, A., Anderson, P. M., Lozhkin, A. V., Bezrukova, E., et al. (2020). A taxonomically harmonized and temporally standardized fossil pollen dataset from Siberia covering the last 40 kyr. *Earth Syst. Sci. Data* 12, 119–135. doi: 10.5194/essd-12-119-2020

Cao, X., Tian, F., Li, F., Gaillard, M.-J., Rudaya, N., Xu, Q., et al. (2019). Pollen-based quantitative land-cover reconstruction for northern Asia covering the last 40 cal ka BP. *Clim. Past* 15, 1503–1536. doi: 10.5194/cp-15-1503-2019

Cao, X.-Y., Herzschuh, U., Telford, R. J., and Ni, J. (2014). A modern pollen–climate dataset from China and Mongolia: assessing its potential for climate reconstruction. *Rev. Palaeobot. Palynol.* 211, 87–96. doi: 10.1016/j.revpalbo.2014.08.007

Cao, X.-Y., Ni, J., Herzschuh, U., Wang, Y.-B., and Zhao, Y. (2013). A late Quaternary pollen dataset from eastern continental Asia for vegetation and climate reconstructions: set up and evaluation. *Rev. Palaeob. Palynol.* 194, 21–37. doi: 10.1016/j.revpalbo.2013.02.003

Carlson, A. E., LeGrande, A. N., Oppo, D. W., Came, R. E., Schmidt, G. A., Anslow, F. S., et al. (2008). Rapid early Holocene deglaciation of the Laurentide ice sheet. *Nat. Geosci.* 1, 620–624. doi: 10.1038/ngeo285

Chang, X., Jin, H., Wang, Y., Zhang, Y., Zhou, G., Che, F., et al. (2012). Influences of vegetation on permafrost: a review. *Acta Ecol. Sin.* 32, 7981–7990.

Chen, F., Xu, Q., Chen, J., Birks, H. J. B., Liu, J., Zhang, S., et al. (2015). East Asian summer monsoon precipitation variability since the last deglaciation. *Sci. Rep.* 5:11186. doi: 10.1038/srep11186

Clift, P. D., and Plumb, R. A. (2008). *The Asian monsoon: Causes, History and Effects*. Cambridge: Cambridge University Press.

Cohen, J. (1994). Snow cover and climate. *Weather* 49, 150–156. doi: 10.1002/j.1477-8696.1994.tb05997.x

Elmendorf, S. C., Henry, G. H., Hollister, R. D., Björk, R. G., Boulanger-Lapointe, N., Cooper, E. J., et al. (2012). Plot-scale evidence of tundra vegetation change and links to recent summer warming. *Nat. Clim. Change* 2, 453–457. doi: 10.1038/nclimate1465

Galushkin, Y. (1997). Numerical simulation of permafrost evolution as a part of sedimentary basin modelling: permafrost in the Pliocene-Holocene climate history of the urengoy field in the West Siberian basin. *Can.J.Earth Sci.* 34, 935–948. doi: 10.1139/e17-078

Guo, D., Liu, T., and Zhang, W. (1998). *Permafrost Institute, Siberian Branch. USSR Academy of Sciences. General Geocryology*. Beijing: Science Press.

Herzschuh, U., Birks, H. J. B., Laepple, T., Andreev, A., Melles, M., and Brigham-Grette, J. (2016). Glacial legacies on interglacial vegetation at the Pliocene-Pleistocene transition in NE Asia. *Nat. Commun.* 7:11967. doi: 10.1038/ncomms11967

Herzschuh, U., Cao, X., Laepple, T., Dallmeyer, A., Telford, R. J., Ni, J., et al. (2019). Position and orientation of the westerly jet determined Holocene rainfall patterns in China. *Nat. Commun.* 10:2376. doi: 10.1038/s41467-019-09866-8

Intergovernmental Panel on Climate Change (2013). "Summary for Policymakers in Climate Change 2013: the Physical Science Basis," in *Contribution of Working Group I to the Fifth Assessment Report of the Intergovernmental Panel on Climate Change*, eds T. F. Stocker, D. Qin, G.-K. Plattner, M. Tignor, S. K. Allen, J. Boschung, et al. (Cambridge: Cambridge University Press).

Intergovernmental Panel on Climate Change (2019). "Summary for Policymakers," in *IPCC Special Report on the Ocean and Cryosphere in a Changing Climate*, eds H.-O. Pörtner, D. C. Roberts, V. Masson-Delmotte, P. Zhai, M. Tignor, E. Poloczanska, et al. (Geneva: Intergovernmental Panel on Climate Change).

Jacob, D., Goettel, H., Jungclaus, J., Muskulus, M., Podzun, R., and Marotzke, J. (2005). Slowdown of the thermohaline circulation causes enhanced maritime climate influence and snow cover over Europe. *Geophys. Res. Lett.* 32:L21711. doi: 10.1029/2005GL023286

Jin, H., Jin, X., He, R., Luo, D., Chang, X., Wang, S., et al. (2019). Evolution of permafrost in China during the last 20 ka. *Sci. China Earth Sci.* 62, 1207–1223. doi: 10.1007/s11430-018-9272-0

Kang, S., Du, J., Wang, N., Dong, J., Wang, D., Wang, X., et al. (2020). Early Holocene weakening and mid-to late Holocene strengthening of the East Asian winter monsoon. *Geology* 48, 1043–1047. doi: 10.1130/g47621.1

Karlsson, J. M., Lyon, S. W., and Destouni, G. (2012). Thermokarst lake, hydrological flow and water balance indicators of permafrost change in Western Siberia. *J. Hydrol.* 464, 459–466. doi: 10.1016/j.jhydrol.2012.07.037

Klemm, J., Herzschuh, U., and Pestryakova, L. (2016). Vegetation, climate and lake changes over the last 7000 years at the boreal treeline in north-central Siberia. *Q. Sci. Rev.* 147, 422–434. doi: 10.1016/j.quascirev.2015.08.015

Knoblauch, C., Beer, C., Liebner, S., Grigoriev, M. N., and Pfeiffer, E.-M. (2018). Methane production as key to the greenhouse gas budget of thawing permafrost. *Nat. Clim. Change* 8, 309–312. doi: 10.1038/s41558-018-0095-z

Landis, J. R., and Koch, G. G. (1977). The measurement of observer agreement for categorical data. *Biometrics* 33, 159–174. doi: 10.2307/2529310

Laskar, J., Robutel, P., Joutel, F., Gastineau, M., Correia, A. C. M., and Levrard, B. (2004). A long-term numerical solution for the insolation quantities of the Earth. *Astronomy Astrophysics* 428, 261–285. doi: 10.1051/0004-6361:20041335

Li, T.-Y., Baker, J. L., Wang, T., Zhang, J., Wu, Y., Li, H.-C., et al. (2021). Early Holocene permafrost retreat in West Siberia amplified by reorganization of westerly wind systems. *Commun. Earth Environ.* 2:199. doi: 10.1038/s43247-021-00238-z

Li, Z. K., Zhu, W. J., and Wu, B. Y. (2011). Impact of improved soil freezing process on climate in East Asia using NCAR CAM model. Chinese. *J. Atmos. Sci. (Chinese)* 35, 683–693. doi: 10.3878/j.issn.1006-9895.2011.04.08

Liaw, A. (2018). *Randomforest: Breiman and Cutler's Random Forests for Classification and Regression, version 4.7-1*. Available online at https://cran.r-project.org/web/packages/randomForest/index.html (accessed March 11, 2022).

Lindgren, A., Lu, Z., Zhang, Q., and Hugelius, G. (2021). Reconstructing past global vegetation with random forest machine learning, sacrificing the dynamic response for robust results. *J. Adv. Model. Earth Syst.* 13:e2020MS002200. doi: 10.1029/2020MS002200

Liu, J., Chen, J., Zhang, X., Li, Y., Rao, Z., and Chen, F. (2015). Holocene east Asian summer monsoon records in northern China and their inconsistency with Chinese stalagmite δ18O records. *Earth Sci. Rev.* 148, 194–208. doi: 10.1016/j.earscirev.2015.06.004

Liu, X., and Yanai, M. (2002). Influence of Eurasian spring snow cover on Asian summer rainfall. *Int. J. Climatol.* 22, 1075–1089. doi: 10.1002/joc.784

Lloyd, A. (2005). Ecological histories from Alaskan tree lines provide insight into future change. *Ecology* 86, 1687–1695. doi: 10.1890/03-0786

Marcott, S. A., Shakun, J. D., Clark, P. U., and Mix, A. C. (2013). A reconstruction of regional and global temperature for the past 11,300 years. *Science* 339, 1198–1201. doi: 10.1126/science.1228026

Meier, E., Lischke, H., Schmatz, D., and Zimmermann, N. E. (2012). Climate, competition and connectivity affect future migration and ranges of European trees. *Glob. Ecol. Biogeogr.* 21, 164–178. doi: 10.1111/j.1466-8238.2011.00669.x

Miller, G. H., Alley, R. B., Brigham-Grette, J., Fitzpatrick, J. J., Polyak, L., Serreze, M. C., et al. (2010). Arctic amplification: can the past constrain the future? *Q. Sci. Rev.* 29, 1779–1790. doi: 10.1016/j.quascirev.2010.02.008

Müller, S., Tarasov, P. E., Andreev, A. A., Tütken, T., Gartz, S., and Diekmann, B. (2010). Late quaternary vegetation and environments in the Verkhoyansk Mountains region (NE Asia) reconstructed from a 50-kyr fossil pollen record from lake billyakh. *Q. Sci. Rev.* 29, 2071–2086. doi: 10.1016/j.quascirev.2010.04.024

Myers-Smith, I. H., Kerby, J. T., Phoenix, G. K., Bjerke, J. W., Epstein, H. E., Assmann, J. J., et al. (2020). Complexity revealed in the greening of the Arctic. *Nat. Clim. Change* 10, 106–117. doi: 10.1038/s41558-019-0688-1

Natali, S. M., Holdren, J. P., Rogers, B. M., Treharne, R., Duffy, P. B., Pomerance, R., et al. (2021). Permafrost carbon feedbacks threaten global climate goals. *Proc. Natl. Acad. Sci.* 118:e2100163118. doi: 10.1073/pnas.2100163118

Natalia, R., Sergey, K., Słowiński, M., Cao, X., and Zhilich, S. (2020). Postglacial history of the steppe Altai: climate, fire and plant diversity. *Q. Sci. Rev.* 249:106616. doi: 10.1016/j.quascirev.2020.106616

Niemeyer, B., Klemm, J., Pestryakova, L. A., and Herzschuh, U. (2015). Relative pollen productivity estimates for common taxa of the northern Siberian Arctic. *Rev. Palaeobot. Palynol.* 221, 71–82. doi: 10.1016/j.revpalbo.2015.06.008

Osawa, A., Zyryanova, O. A., Matsuura, Y., Kajimoto, T., and Wein, R. W. (2010). *Permafrost Ecosystems: Siberian Larch Forests*. Berlin: Springer, 502.

Prasad, A. M., Iverson, L. R., and Liaw, A. (2006). Newer classification and regression tree techniques: bagging and random forests for ecological prediction. *Ecosystems* 9, 181–199. doi: 10.1007/s10021-005-0054-1

Qin, F. (2021). Modern pollen assemblages of the surface lake sediments from the steppe and desert zones of the Tibetan Plateau. *Sci. China Earth Sci.* 64, 425–439. doi: 10.1007/s11430-020-9693-y

R Core Team (2020). *R: A Language and Environment For Statistical Computing*. Vienna: R Foundation for Statistical Computing.

Schaeffer, M., Eickhout, B., Hoogwijk, M., Strengers, B., Vuuren, D., Leemans, R., et al. (2006). CO_2 and albedo climate impacts of extratropical carbon and biomass plantations. *Global Biogeochem. Cycles* 20:GB2020. doi: 10.1029/2005GB002581

Schulze, E.-D., Wirth, C., Mollicone, D., von Lüpke, N., Ziegler, W., Achard, F., et al. (2012). Factors promoting larch dominance in central Siberia: fire versus growth performance and implications for carbon dynamics at the boundary of evergreen and deciduous conifers. *Biogeosciences* 9, 1405–1421. doi: 10.5194/bg-9-1405-2012

Shakun, J. D., Clark, P. U., He, F., Marcott, S. A., Mix, A. C., Liu, Z., et al. (2012). Global warming preceded by increasing carbon dioxide concentrations during the last deglaciation. *Nature* 484, 49–54. doi: 10.1038/nature10915

Shuman, J. K., Shugart, H. H., and O'Halloran, T. L. (2011). Sensitivity of Siberian larch forests to climate change. *Glob. Change Biol.* 17, 2370–2384. doi: 10.1111/j.1365-2486.2011.02417.x

Streletskaya, I., Gusev, E., Vasiliev, A., Oblogov, G., and Molodkov, A. (2013). Pleistocene-Holocene palaeoenvironmental records from permafrost sequences at the Kara Sea coast (NW Siberia, Russia). *Geogr. Environ. Sustain.* 6, 60–76. doi: 10.24057/2071-9388-2013-6-3-60-76

Strobl, C., Boulesteix, A. L., Zeileis, A., and Hothorn, T. (2007). Bias in random forest variable importance measures: Illustrations, sources and a solution. *BMC Bioinformatics* 8:25. doi: 10.1186/1471-2105-8-25

Tarasov, P. E., Nakagawa, T., Demske, D., Österle, H., Igarashi, Y., Kitagawa, J., et al. (2011). Progress in the reconstruction of Quaternary climate dynamics in the northwest Pacific: a new modern analogue reference dataset and its application to the 430-kyr pollen record from lake biwa. *Earth Sci. Rev.* 108, 64–79. doi: 10.1016/j.earscirev.2011.06.002

Tchebakova, N. M., Rehfeldt, G. E., and Parfenova, E. I. (2006). Impacts of climate change on the distribution of *Larix* spp. and pinus sylvestris and their climatypes in Siberia. *Mitig. Adapt. Strateg. Glob. Change* 11, 861–882. doi: 10.1007/s11027-005-9019-0

Tian, F., Cao, X., Dallmeyer, A., Lohmann, G., Zhang, X., Ni, J., et al. (2018). Biome changes and their inferred climatic drivers in northern and eastern continental Asia at selected times since 40 cal ka BP. *Veg. Hist. Archaeobot.* 27, 365–379. doi: 10.1007/s00334-017-0653-8

Travis, J., Delgado, M., Bocedi, G., Baguette, M., Bartoń, K., Dries, B., et al. (2013). Dispersal and species' responses to climate change. *Oikos* 122, 1532–1540. doi: 10.1111/j.1600-0706.2013.00399.x

Tyrtikov, A. (1973). "Permafrost and vegetation," in *Permafrost Second International Conference: Proceedings*, ed. F. J. Sanger (Washington D.C: National Academy of Sciences), 100–103.

Tzedakis, P. C., and Bennett, K. D. (1995). Interglacial vegetation succession: a view from southern Europe. *Q. Sci. Rev.* 14, 967–982. doi: 10.1016/0277-3791(95)00042-9

Vaks, A., Gutareva, O. S., Breitenbach, S. F., Avirmed, E., Mason, A. J., Thomas, A. L., et al. (2013). Speleothems reveal 500,000-year history of Siberian permafrost. *Science* 340, 183–186. doi: 10.1126/science.1228729

Vaks, A., Mason, A. J., Breitenbach, S. F. M., Kononov, A. M., Osinzev, A. M., Rosensaft, M., et al. (2020). Palaeoclimate evidence of vulnerable permafrost during times of low sea ice. *Nature* 577, 221–225. doi: 10.1038/s41586-019-1880-1

Vasiliev, A. A., Drozdov, D. S., Gravis, A. G., Malkova, G. V., Nyland, K. E., and Streletskiy, D. A. (2020). Permafrost degradation in the western Russian Arctic. *Env. Res. Lett.* 15:045001. doi: 10.1088/1748-9326/ab6f12

Velichko, A. A., Wright, H. E., and Barnosky, C. W. (eds) (1984). *Late Quaternary Environments of the Soviet Union*. Minneapolis, MN: University of Minnesota Press, 87–91.

Wang, B. (2006). *The Asian Monsoon*. Berlin: Springer.

Wang, P., Huang, Q., Pozdniakov, S. P., Liu, S., Ma, N., Wang, T., et al. (2021). Potential role of permafrost thaw on increasing Siberian river discharge. *Env. Res. Lett.* 16:034046. doi: 10.1088/1748-9326/abe326

Washburn, A. L. (1973). *Periglacial Processes and Environments*. London: Edward Arnold.

Wu, B., Yang, K., and Zhang, R. (2009). Eurasian snow cover variability and its association with summer rainfall in China. *Adv. Atmos. Sci.* 26, 31–44. doi: 10.1007/s00376-009-0031-2

Xiao, J., Xu, Q., Nakamura, T., Yang, X., Liang, W., and Inouchi, Y. (2004). Holocene vegetation variation in the Daihai Lake region of north-central China: a direct indication of the Asian monsoon climatic history. *Q. Sci. Rev.* 23, 1669–1679. doi: 10.1016/j.quascirev.2004.01.005

Xin, Y., Wu, B., Bian, L., Liu, G., Zhang, L., and Li, R. (2012). Response of the East Asian climate system to water and heat changes of global frozen soil using NCAR CAM model Chinese. *Sci. Bull.* 57, 4462–4471. doi: 10.1007/s11434-012-5361-2

Xu, B., Chen, H., Gao, C., Zeng, G., and Huang, Q. (2021). Abnormal change in spring snowmelt over Eurasia and its linkage to the East Asian summer monsoon: The hydrological effect of snow cover. *Front. Earth Sci.* 8:486. doi: 10.3389/feart.2020.594656

Xu, Z., Mason, J. A., Xu, C., Yi, S., Bathiany, S., Yizhaq, H., et al. (2020). Critical transitions in Chinese dunes during the past 12,000 years. *Sci. Adv.* 6:eaay8020. doi: 10.1126/sciadv.aay8020

Yang, S., and Xu, L. (1994). Linkage between Eurasian winter snow cover and regional Chinese summer rainfall. *Int. J. Climatol.* 14, 739–750. doi: 10.1002/joc.3370140704

Yu, S.-Y., Colman, S. M., Lowell, T. V., Milne, G. A., Fisher, T. G., Breckenridge, A., et al. (2010). Freshwater outburst from Lake Superior as a trigger for the cold event 9300 years ago. *Science* 328, 1262–1266. doi: 10.1126/science.1187860

Zhang, H. (1983). "Preliminary studies on relationships between vegetation and frozen ground in Da Hinggan forest area (in Chinese)," in *Proceedings of the 2nd National Conference on Permafrost* (Lanzhou: Gansu People's Publishing House), 81–84.

Zhang, Q., and Chen, J. (2020). Enhanced East Asian summer monsoon precipitation due to vegetation feedback during the last interglacial 127 ka. *Q. Sci.* 40, 1499–1512. doi: 10.11928/j.issn.1001-7410.2020.06.11

Zhang, T., Barry, R. G., Knowles, K., Heginbottom, J., and Brown, J. (1999). Statistics and characteristics of permafrost and ground-ice distribution in the Northern Hemisphere. *Polar Geogr.* 23, 132–154. doi: 10.1080/10889379909377670

Conflict of Interest: The authors declare that the research was conducted in the absence of any commercial or financial relationships that could be construed as a potential conflict of interest.

Publisher's Note: All claims expressed in this article are solely those of the authors and do not necessarily represent those of their affiliated organizations, or those of the publisher, the editors and the reviewers. Any product that may be evaluated in this article, or claim that may be made by its manufacturer, is not guaranteed or endorsed by the publisher.